

COMBINATORIAL INVESTIGATIONS OF POLYMER ADHESION

Alfred J. Crosby, Alamgir Karim, Eric J. Amis

Polymers Division
National Institute of Standards and Technology
Gaithersburg, MD 20899-8542

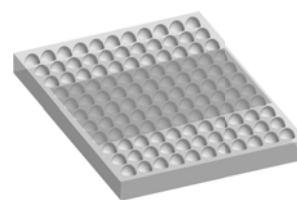


Figure 1. Schematic of PDMS microlens array. Center five rows are shown with floated PS coating.

Introduction

Polymer adhesion is important to numerous technologies including electronic packaging, coatings and paints, biomedical implants, and pressure-sensitive adhesives. In all of these application areas, the prescribed degree of polymer adhesion is largely dependent upon the end-use environment/application of the technology. For example, in electronic packaging the structural integrity of the package is directly dependent upon the interfacial strength of multiple polymer interfaces. These interfaces must maintain their strength under large temperature fluctuations and large mechanical strains. In contrast, many polymers in biomedical implants require non-adhesive surfaces to minimize contamination. The design of specific polymer systems for such diverse applications requires a thorough understanding of the molecular physics and chemistry governing the adhesion.

From current knowledge, it is well known that polymer adhesion is dependent upon a multitude of variables ranging from surface chemistry to bulk viscoelastic properties and from temperature to thickness of the adhesive layer.¹ Given the time required in using conventional experimental methods to quantitatively investigate polymer adhesion, it is difficult to obtain a broad understanding of polymer adhesion and the effect of multivariable environments on this property. This difficulty not only limits fundamental pursuit for developing predictive models to describe adhesive processes, but conventional experimental methods also limit the selection process used in industry to identify optimal candidates for a specific adhesive application. To alleviate these challenges, our research builds on the framework in the pharmaceutical industry which uses combinatorial methodology to pursue drug optimization.² Although its roots in the pharmaceutical industry, and its introduction into the materials science field, have focused on the synthesis of optimized compounds³, combinatorial methodology is equally powerful for characterizing material properties and nurturing our understanding of fundamental materials physics.

In this work, we introduce a combinatorial technique that can be used to investigate adhesive interactions between a polymer and either another polymer, a ceramic, or a metal. The primary goal in the development of this technique is to design a high-throughput, parallel processing adhesion test that allows the adhesive strength dependence on multivariable environments to be determined. This combinatorial polymer adhesion test will provide qualitative and quantitative data used to determine absolute measures of adhesion as a function of the multidimensional parameter space. These results will aid industrial screening for optimal adhesives, as well as provide a unique tool for gaining a fundamental understanding of polymer adhesion.

We investigate the temperature and thickness dependence of the self-adhesion of polystyrene (PS) and the adhesion between PS and poly(dimethylsiloxane) (PDMS) for demonstration of concept.

Experimental

Combinatorial methodology involving library generation, library evaluation, and data assessment are discussed.

Library Generation. Our libraries consist of an array of microlenses as illustrated in Figure 1. For the research described here, the material of the microlens array is PDMS, Dow Corning's Sylgard 184⁴ mixed in a 10:1 ratio of base to curing agent. After curing the PDMS microlenses at room temperature for 48 h, the samples were swollen in heptane for 12 h to remove any uncrosslinked chains and subsequently air dried for 30 h and under vacuum for 2.5 h at 60°C. A thin layer of PS, prepared by flow coating to allow both uniform and gradient thickness films, was floated onto a region of the microlens array as illustrated in Figure 1. The flow coating technique has been published previously.⁵

For the complementary surface, we flow coated a piranha-etched Si wafer with a thin, uniform layer of PS of 30 nm. The molecular mass of the PS used to coat both the Si wafer and the microlens array is 114,200 g/mol.⁶ The temperature dependence of the adhesive strength was studied by placing the coated Si onto a heating stage that can be used to produce uniform or linear temperature gradients across the sample. Details regarding this apparatus have been published previously.⁵

Library Evaluation. To evaluate the adhesion between the microlens library and the coating of the Si wafer, we use "contact and separation". In this process, the two library components are moved into normal contact with a vertically-positioned actuator that is fixed to an automated X-Y translation stage mounted on a Nikon Optiphot⁴ optical microscope. The two library components continue to be moved toward each other at a relative velocity of 1.0 μm/s until an arbitrarily-chosen maximum contact point is reached. At this point, the direction of the two components is reversed, and the two components are separated at a constant velocity. The separation process continues until the contact area of all microlenses is equal to zero. We use Labview⁴ software to control the motion of the actuator, to record the displacement readings of the actuator's linear encoder, and to collect the images of contact areas between the microlens array and the coated Si substrate.

Data Assessment. The results of this test are two fold. First, the images of the contact areas yield a qualitative map of the relative adhesion differences of the interfaces created across the microlens array. For instance, if the two library components are ideally parallel and the initial point of contact is the same for every microlens, then, upon separation, the microlens interfaces that release contact first have the weakest adhesion, while those contact areas that release last possess the greatest adhesive strength. If the two components are not ideally aligned, qualitative mappings are still possible by comparing the order of contact to the order of separation. If the adhesive strength is uniform across the microlens, then the order of contact will mirror the order of separation. The relative adhesion values can be inferred from deviations from this mirroring.

Second, the displacement (δ) and contact radius (a) of each individual microlens is measured. This data is called a contact history and can be used to determine the adhesion energy of the interface. To determine the adhesion energy of each interface, we build upon the theory of Johnson, Kendall, and Roberts (JKR).⁷ This theory describes how the adhesion energy of elastic systems can be quantified from the deviation of the actual contact radius from that predicted by classical Hertzian contact mechanics. Briefly, the JKR theory yields the following equation to describe the contact radius, a , as a function of the applied force, P , the work of adhesion, G , the elastic modulus, E , and the radius of curvature of the contacting lens, R :⁷

$$a^3 = \frac{9R}{16E} \left[P + 3\pi GR + \sqrt{6GRP + (3\pi GR)^2} \right] \quad (1)$$

This equation and the JKR theory are only valid when the contact radius is significantly less than all other length scales in the test geometry. As Gent, Maugis, and others demonstrated, equation (1) can be rewritten in the form of a conventional fracture mechanics relation:^{8,9}

$$G = \frac{3(P' - P)^2}{32\pi E \cdot a^3} \quad (2)$$

where P' is the required force to establish a contact radius of a in the absence of adhesion, or $P' = 16Ea^3/9R$ in the limit of an incompressible material. For our combinatorial adhesion measurement, the contact force of each microlens

is not directly measured, but the displacement is recorded. If our contacting bodies behave as linear elastic solids, then equation (2) can be rewritten as:¹⁰

$$G = \frac{2E(\delta' - \delta)^2}{3\pi a} \quad (3)$$

by using the definition of compliance, C :

$$C = \frac{d\delta}{dP} = \frac{\delta' - \delta}{P' - P} = \frac{3}{8Ea} \quad (4)$$

where δ' is the required displacement to establish a contact radius of a in the absence of adhesion, or $\delta' = a^2/R$. Therefore, using equation (3), the adhesion energy, G , can be calculated from the contact history of each microlens if the underlying assumptions of the JKR theory are satisfied. For cases where viscoelasticity or finite size effects play a dominant role, modifications to the JKR theory can be used to quantify the adhesion energy.^{10,11}

Results and Discussion

We investigated the differences between the self-adhesion of PS and the adhesion between PS and PDMS combinatorially. Using the partially coated microlens array illustrated schematically in Figure 1, as the two library components are contacted and separated, two different interfaces are created. For the microlenses coated with a thin layer of PS, the interface is PS/PS. On either side of this strip of PS coating, the measured interface is PS/PDMS.

In the first tests, the thickness of the PS coating on the microlens array is 30 nm. The quantitative contact history for two individual microlenses is shown in Figure 2. As evident in Figure 2, the difference in adhesion between the two interfaces at room temperature is negligible. In contrast, at a temperature near 80°C, the self-adhesion of PS is significantly greater than the adhesion of the PS/PDMS interface. This increase in adhesion is due to the diffusion of surface PS chains across the interface causing molecular entanglement. In fact, this interface is strong enough to fracture the PS coating of the microlens around the perimeter of contact. This fracturing leaves "weld" spots deposited onto the PS coating of the Si wafer (Figure 3)).

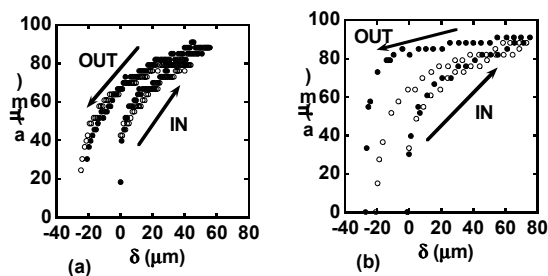


Figure 2. Contact radius versus displacement for two representative microlenses. Filled circles represent PS/PS interface. Open circles represent PS/PDMS interface. (a) $T = 25^\circ\text{C}$. (b) $T = 80^\circ\text{C}$.

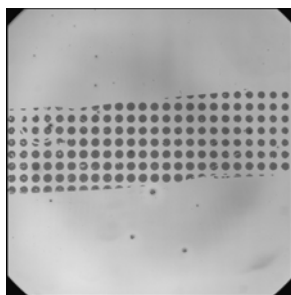


Figure 3. Image of PS "weld" spots after final separation, for a floated PS layer of 30 nm and uniform temperature of PS coated Si of 80°C.

To further investigate strength development of the PS/PS interface, we can use combinatorial methods to determine the critical temperature for the PS "weld" spots to occur. By applying a temperature gradient along the array of interfaces, we find that the critical temperature to develop the required

interfacial strength is 76°C for a floated 30 nm thick PS layer (Figure 4(a)). If the thickness of the floated PS layer is increased to 215 nm, the critical temperature shifts to 89°C (Figure 4(b)). These results suggest a thickness dependence of the critical temperature for PS welding. Therefore, in our future work we can use the true power of combinatorial methods and can create one sample with a thickness gradient in one direction and a temperature gradient applied in the orthogonal direction. This configuration will allow the overall dependence of critical welding temperature on thickness to be determined within a single test.

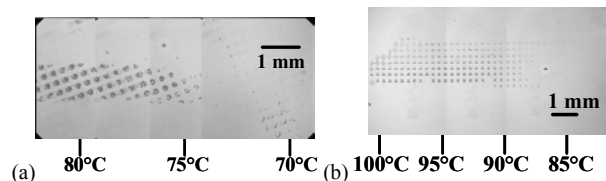


Figure 4. Images of PS weld spots left on PS coated Si wafer after contact and separation of microlens array. Thickness of floated PS layer is (a) 30 nm and (b) 215 nm.

Conclusions

We have developed a combinatorial technique to investigate the dependence of polymer adhesion on multidimensional parameter space. This technique can be applied to polymer to polymer, polymer to ceramic, and polymer to metal interfaces. In this initial work, we have used the combinatorial adhesion test to map the effect of thickness on the critical temperature for PS to PS welding.

Acknowledgement. Support from the National Research Council (A.J.C.) is acknowledged.

References

- (1) Zosel, A. *Colloid and Polymer Science* **1985**, 263, 541-553.
- (2) Brocchini, S.; James, K.; Tangpasuthadol, V.; Kohn, J. J. *Biomed. Mater. Res.* **1998**, 42, 66.
- (3) Jandeleit, B.; Schaefer, D. J.; Powers, T. S.; Turner, H. W.; Weinberg, W. H. *Angew. Chem. Int. Ed.* **1999**, 38, 2494-2532.
- (4) Certain equipment and instruments or materials are identified in the paper to adequately specify the experimental details. Such identification does not imply recommendation by NIST.
- (5) Meredith, J. C.; Karim, A.; Amis, E. J. *Macromolecules* **2000**, 33, 5760-5762.
- (6) According to ISO 31-8, the term "molecular weight" has been replaced by "relative molecular mass", M_r . The conventional notation, rather than the ISO notation, has been employed for this publication.
- (7) Johnson, K. L.; Kendall, K.; Roberts, A. D. *Proc. R. Soc. Lond. A* **1971**, 324, 301-313.
- (8) Gent, A. N.; Petrich, R. P. *Proc. Roy. Soc. A* **1969**, 310, 433-448.
- (9) Maugis, D.; Barquins, M. *J. Phys. D: Appl. Phys.* **1978**, 11, 1989-2023.
- (10) Shull, K. R.; Ahn, D.; Chen, W.-L.; Flanigan, C. M.; Crosby, A. J. *Macromol. Chem. Phys.* **1998**, 199, 489-511.
- (11) Lin, Y. Y.; Hui, C. Y.; Baney, J. M. *Journal of Applied Physics* **1999**, 85, 2250-2260.